

# TNF- $\alpha$ Impairs Pericyte-Mediated Cerebral Microcirculation via the NF- $\kappa$ B/iNOS Axis After Experimental Traumatic Brain Injury

**Shaorui Zheng**

Department of Neurosurgery, Fuzong Clinical Medical college, Fujian Medical University

**Cheng Wang**

Department of Neurosurgery, the First Affiliated Hospital of Wannan Medical college

**Long Lin**

Department of Neurosurgery, Fuzong clinical Medical college, Fujian Medical University

**Shuwen Mu**

Department of Neurosurgery, Fuzong Clinical Medical college, Fujian Medical University

**Haibing Liu**

Department of Neurosurgery, 900th Hospital

**Xiaofang Hu**

Department of Neurosurgery, 900th Hospital

**Xiangrong Chen** (✉ [rong281@126.com](mailto:rong281@126.com))

Second Affiliated Hospital of Fujian Medical University <https://orcid.org/0000-0001-9400-7358>

**Shousen Wang**

Department of Neurosurgery, Fuzong Clinical Medical college, Fujian Medical University

---

## Research

**Keywords:** Traumatic brain injury, Pericyte, Microglia, Neurovascular unit, Microcirculation, Neuroinflammation, Oxidative stress, TNF- $\alpha$ /NF- $\kappa$ B/iNOS pathway.

**Posted Date:** November 2nd, 2021

**DOI:** <https://doi.org/10.21203/rs.3.rs-1008540/v1>

**License:**  This work is licensed under a Creative Commons Attribution 4.0 International License.

[Read Full License](#)

---

# Abstract

## Background

Secondary structural and functional abnormalities of the neurovascular unit are important pathological mechanisms following traumatic brain injury (TBI). The tumor necrosis factor  $\alpha$  (TNF- $\alpha$ )/nuclear factor- $\kappa$ B (NF- $\kappa$ B) pathway regulates neuroinflammation and oxidative damage, which may act as triggers for pathological processes after TBI. However, the role of TNF- $\alpha$ /NF- $\kappa$ B in pericyte-mediated cerebral microcirculation are currently unknown.

## Methods

We assessed the activity and mechanisms of the TNF- $\alpha$ /NF- $\kappa$ B signaling axis on pericyte-mediated microcirculation using the mouse controlled cortical impact model and BV2 cells. Immunofluorescent staining and western blot analysis were used to detect activation of the TNF- $\alpha$ /NF- $\kappa$ B signaling pathway and the expression of inducible nitric oxide synthase (iNOS) to evaluate the effects of the TNF- $\alpha$  specific inhibitor infliximab (IFX). Modified neurological severity scores, Garcia test, Nissl staining, and TUNEL staining were employed to determine the neuroprotective effects of IFX supplementation. The relative blood flow values in the capillary areas surrounding the impinging lesion were observed by Laser speckle contrast imaging. The impact of IFX on pericyte markers was assessed to evaluate whether pericyte damage was dependent on the TNF- $\alpha$ /NF- $\kappa$ B/iNOS axis to gain further insight into the mechanisms underlying the development of the microcirculation disturbance after TBI.

## Results

Microglia were activated after TBI, and the expression of NF- $\kappa$ B, iNOS, a disintegrin and metalloproteinase 17, inflammatory factors, and free radicals increased around the injury areas. After lipopolysaccharide treatment, the expression of TNF- $\alpha$  and downstream NF- $\kappa$ B/iNOS in BV2 cells was significantly upregulated. Pharmacological inhibition of TNF- $\alpha$  via IFX significantly reduced NF- $\kappa$ B p65 phosphorylation and nuclear translocation and downregulated iNOS expression. Meanwhile, we found that specific inhibition of TNF- $\alpha$  reversed pericyte marker loss, and improved pericyte function and cerebral microcirculation perfusion after TBI, which could attenuate inflammation and oxidative damage, reduce neuronal cell damage and apoptosis, and play a neuroprotective role.

## Conclusion

The results of this study suggested that microglia activated and released TNF- $\alpha$  after TBI, which promoted neuroinflammation and oxidative stress by activating downstream NF- $\kappa$ B/iNOS signals, and

this led to pericyte-mediated disturbance of the cerebral microcirculation, which may be one of the vital mechanisms of secondary injury in TBI.

## Background

Secondary injury induced by traumatic brain injury (TBI) is considered to be a reversible pathological process, which involves vascular, cellular, metabolic, molecular, and other factors, of which neuroinflammation and oxidative stress are the key links[1-3]. In the past, TBI research focused on neurons, ignoring the role of glia, and the cerebrovascular system[4]. After the concept of the neurovascular unit (NVU) was proposed, people gradually realized that neurons, blood vessels, and glia as a whole maintain homeostasis and the function of the central nervous system (CNS) through crosstalk[5-7]. The conceptual framework of the NVU may contribute to understanding the pathophysiological changes of TBI. Recent studies have demonstrated that the NVU is a key participant in secondary injury following TBI[8, 9].

The NVU is composed of neurons, microglia, astrocytes, pericytes, smooth muscle cells, and endothelial cells. It is the minimum acting unit necessary to maintain the proper function of the CNS[10]. The NVU maintains blood brain barrier (BBB) and vascular integrity through the interaction between its constituent cells[11]. After TBI, microvascular dysfunction is mainly manifested by NVU dysfunction, which is regulated by pericyte function[12]. Pericytes are microvascular mural cells distributed in precapillary arteries, capillaries, and postcapillary venules[13]. In the NVU, pericytes interact with neighboring cells and process signals to execute multiple functional responses, particularly to the regulation of the microvessels[14]. Recent studies have shown that pericyte degeneration after TBI led to regional microcirculatory hypoperfusion and an increase of BBB permeability, which mediated microcirculation disturbance[15-17]. A deeper exploration of pericyte-mediated microcirculation disorders is essential to investigate the pathological mechanisms following TBI.

An increasing body of evidence shows that the pericyte-mediated microcirculation function is influenced by neuroinflammation[18, 19]. Microglia are the major immunocompetent cells in the NVU, and their activation is a hallmark of neuroinflammation[6, 20]. After the initial injury, the altered microenvironment and intracellular components released from damaged cells trigger local glial activation and recruitment[5]. Activated microglia induce neuroinflammation and aggravate tissue damage by promoting the release of inflammatory factors, inflammatory cell infiltration, as well as free radical production[21, 22]. The generated free radicals not only induce oxidative stress but also act as an inflammatory mediator to amplify inflammation[2]. In the brain, a large pool of microglia (also known as perivascular microglia) are located at the proximal region surrounding the cerebrovasculature. Moreover, confocal laser scanning microscopy analysis revealed the highest density of microglial endfeet contacting the glial basement membrane around capillaries, with significantly lower densities around arteries and veins. These structural features allow a close interaction between microglia and pericytes. Indeed, many studies have demonstrated a very tight spatiotemporal correlation between vascular

activation, cerebral blood flow (CBF) restriction, BBB breakdown, and activation of brain-resident microglia[23-25].

Under pathological conditions, the inflammation-related tumor necrosis factor  $\alpha$  (TNF- $\alpha$ )/nuclear factor- $\kappa$ B (NF- $\kappa$ B) pathway is activated, which is closely related to the prognosis of TBI[26, 27]. TNF- $\alpha$  activates IKK- $\alpha/\beta$  by binding to its receptor, causing I $\kappa$ B phosphorylation and promoting NF- $\kappa$ B nuclear translocation, which in turn regulates NF- $\kappa$ B-related signaling pathways[27]. As a pro-inflammatory signal, the TNF- $\alpha$ /NF- $\kappa$ B pathway plays a central role in initiating and regulating the cascade of inflammatory factors[28, 29]. In addition, TNF- $\alpha$ /NF- $\kappa$ B can also participate in the inflammatory process of diseases by inducing oxidative stress[30-32]. The overactivated inflammatory response after TBI releases abundant inflammatory factors, induces oxidative stress, and produces excessive oxidative free radicals including reactive oxygen species (ROS) and reactive nitrogen species (RNS). Inducible nitric oxide synthase (iNOS), a subtype of nitric oxide synthase that is only induced under pathological conditions, is regulated by NF- $\kappa$ B. When iNOS is activated, it can release a large amount of NO, which leads to the excessive production of ROS/RNS[33-36]. In the brain, the unchecked ROS/RNS release leads to lipid peroxidation of cell membranes. This in turn disrupts phospholipid-dependent enzymes and ionic gradients resulting in other sequelae, including disturbances of the CBF, BBB permeability changes, and the development of edema[33]. Among the many studies concerning the role(s) of ROS/RNS molecules are those that have demonstrated their major role in the signal transduction pathways associated with vascular contraction and relaxation[33, 37]. Oxidative stress triggered by free radicals is closely associated with the functional regulation of vascular cells, including endothelial cells and pericytes. Free radicals, particularly RNS can impair pericyte function, stimulating pericyte contraction. Subsequently, the contracted pericytes die upon further activity of damaging factors, leading to sustained constriction of the microvasculature and affecting local blood perfusion[33, 38, 39].

Considering that the TNF- $\alpha$ /NF- $\kappa$ B/iNOS pathway is an important regulatory factor of the neuroinflammatory response, it may be closely related to pericyte-mediated microcirculation. Therefore, we speculated that the activation of the TNF- $\alpha$ /NF- $\kappa$ B/iNOS pathway after TBI promoted neuroinflammation and oxidative stress, which may impair cerebral microcirculation by affecting the function of pericytes.

## Methods

### Animals

All animal experiments were approved by the 900th Hospital Ethics Committee (Fuzhou, China) and were performed under strict supervision. Adult male C57BL/6 mice ( $25 \pm 3$ g) were purchased from the experimental animal facilities of Fujian Medical University. All animals were housed at room temperature (24–26 °C), with a light-dark cycle of 10 h/14 h, and were provided with sufficient water and food.

### Experimental model and drug administration

All mice were randomly divided into three groups: a control group, a TBI group, and a TBI+infliximab (IFX) group (n = 18 each). Nine mice in each group were used for neurological assessment and cerebral blood flow monitoring, and the remaining mice were used for histological and molecular studies. The details of the damage caused by controlled cortical impact (CCI) have been described previously[40]. First, anesthesia was induced with 3% isoflurane in a plexiglass container. After the animal was successfully anesthetized, anesthesia was maintained with 1.5% isoflurane delivered using a small-animal anesthetic machine (RWD Life Science Co., Shenzhen, China). Then each mouse was placed in a stereotactic frame. The craniotomy was located approximately midway between bregma and lambda on the right side, with the medial edge of the craniotomy 1 mm lateral to the midline. Mice were subjected to an impact using a 2 mm metal flat-tip impactor (Brain and Spinal Cord Impactor, 68099H, RWD Life Science). The impact central point was drilled 2.5 mm to the right of the sagittal suture and 2.5 mm posterior to the coronal suture. The velocity was 5 m/s, the depth was 3 mm, and the impact duration was 100 ms. Then the scalp was closed with a suture, and the mice were put back into their home cages to recover from the anesthesia. The control group animals received identical surgical procedures without CCI. Pharmacological inhibition of TNF- $\alpha$  was performed using IFX, as previously described[41]. Approximately 30 min after TBI, the TBI+IFX group was intraperitoneally injected with IFX (10  $\mu$ g/g, cilag Ag) once per day for 3 consecutive days. The remaining groups were injected with the same dose of the vehicle as used in the TBI+IFX group.

## **Cell culture**

The murine microglial cell line BV2 was obtained from the China Infrastructure of Cell Line Resources (Beijing, China) and cultured in a medium comprising 90% Dulbecco's Modified Eagle's Medium (Invitrogen, Frederick, MD, USA), 10% fetal bovine serum (Hyclone, Logan, UT, USA), and 1% antibiotics (100 U/mL penicillin and 100  $\mu$ g/mL streptomycin) at 37 °C in a humidified atmosphere of 5% CO<sub>2</sub>.

## **Preparation of paraffin-embedded sections**

At 72 h after TBI, after deep anesthesia with sodium pentobarbital, the mice were transcardially perfused with 0.01 M phosphate buffered saline (PBS; pH 7.4) followed by 4% paraformaldehyde solution. Then, the brains were removed and post-fixed by immersion in the same fixative solution at 4 °C for 24–48 h. After dehydration and vitrification, tissue samples were embedded in paraffin, and 4- $\mu$ m sections were prepared. The sections were then dewaxed in xylene, rehydrated in graded ethanol and deionized water, and then processed for immunofluorescence, immunohistochemistry, Nissl staining, and terminal deoxynucleotidyl transferase dUTP nick-end labeling (TUNEL) staining.

## **Immunohistochemical analysis**

Formaldehyde-fixed specimens were embedded in paraffin and cut into 4- $\mu$ m-thick sections that were deparaffinized with xylene and rehydrated in a graded series of alcohol. Antigen retrieval was carried out by microwaving in citric acid buffer. Sections were incubated with an antibody against ionized calcium-binding adapter molecule (Iba)-1 (1:500; Abcam, Cambridge, UK), ADAM17 (1:200; Boasoen

Biotechnology, Beijing, China), NF- $\kappa$ B p65 (1:200; Santa Cruz), or iNOS (1:250; Abcam), washed and then incubated with secondary antibody for 1 h at room temperature. A total of five sections from each animal was used for quantification, and the signal intensity was evaluated as follows[22]: 0, no positive cells; 1, very few positive cells; 2, moderate number of positive cells; 3, large number of positive cells; and 4, the highest number of positive cells.

### **Enzyme-linked immunosorbent assay (ELISA)**

Inflammatory factors and free radicals were measured in brain tissue using ELISA kits (Jingmei Biotechnology, Jiangsu, China) for TNF- $\alpha$ , interleukin (IL)-1 $\beta$ , IL-6, interferon (IFN)- $\gamma$ , ROS, RNS, and cyclic guanosine monophosphate (cGMP). According to the manufacturer's instructions, standards and samples were sequentially incubated with respective monoclonal antibodies, biotinylated anti-rat antibodies, and then horseradish peroxidase. The detected optical density (OD) values were transformed into a concentration.

### **Immunofluorescence staining**

Formaldehyde-fixed specimens were embedded in paraffin and cut into 4- $\mu$ m-thick sections that were deparaffinized with xylene and rehydrated in a graded series of alcohol, followed by antigen retrieval. Sections were incubated overnight at 4 °C with antibodies against Iba-1 (1:500; Abcam), TNF- $\alpha$  (1:100; Abcam), CD31 (1:200, Abcam), NeuN (1:500; Abcam), NF- $\kappa$ B p65 (1:200; Santa Cruz), iNOS (1:250; Abcam),  $\alpha$ -smooth muscle actin ( $\alpha$ -SMA; 1:500; Cell Signaling Technology, Danvers, MA, USA), ZO-1 (1:200; Abcam), or occludin (1:100; Abcam). After washing, the sections were incubated with secondary antibodies for 1 h at room temperature. Cell nuclei were stained with 4',6-diamidino-2-phenylindole (DAPI). Images were captured with a fluorescence microscope (Leica, Wetzlar, Germany).

For the lipopolysaccharide (LPS) group, BV2 cells were stimulated with LPS (0.5  $\mu$ g/mL) for 24 h, while the control group was not treated with LPS. Then the coverslips were washed with PBS three times and fixed with 4% paraformaldehyde for 10 min at room temperature. Then BV2 cells were fixed with 4% paraformaldehyde for 30 min, permeabilized with 0.1% Triton X-100 for 10 min, blocked with 5% bovine serum albumin (BSA) for 60 min, and incubated overnight with primary antibodies against Iba-1 (1:500; Abcam) and TNF- $\alpha$  (1:100; Abcam). After incubation with the secondary antibody and DAPI, images were captured with a fluorescence microscope (Leica, Wetzlar, Germany).

### **Cytokine measurements**

The supernatants were collected, and the concentrations of the cytokine TNF- $\alpha$  were measured using an ELISA kit (Jingmei Biotechnology) according to the manufacturer's instructions.

### **Western blot analysis**

Cultured cells were lysed with radioimmunoprecipitation assay (RIPA) lysis buffer (Santa Cruz Biotechnology), then supplemented with protease and phosphatase inhibitors, scraped off the flasks, and

collected for protein extraction. Tissue samples were collected around the injury from the cortex and were extracted with RIPA lysis buffer. Lysates were incubated on ice and supernatants were collected after centrifugation. The protein concentration was determined using a BCA protein assay kit (Abcam). Then 30 µg of total protein was loaded on a gel and separated by sodium dodecyl sulfate-polyacrylamide gel electrophoresis. Subsequently proteins were transferred to polyvinylidene difluoride membranes and probed with primary antibodies against NFκB p65 (1:500; Santa Cruz), p-NFκB p65 (1:500; Santa Cruz), iNOS (1:500; Abcam), 3-nitrotyrosine (3-NT; 1:3,000; Abcam), α-SMA (1:1,000; Cell Signaling Technology), cleaved caspase3 (1:3,000; Abcam), Bax (1:1,000; Abcam), Bcl2 (1:2,000; Abcam), platelet derived growth factor receptor (PDGFR) β (1:1,000; Abcam), neuron-gial (NG) 2 (1:1,000; Abcam), ZO-1 (1:500; Abcam), occludin (1:1,000; Abcam), claudin-5 (1:500; Thermo Fisher Scientific, Waltham, MA, USA), or aquaporin (AQP) 4 (1:1,000; Abcam) followed by incubation with appropriate horseradish peroxidase-conjugated IgG (1:5,000, Boster Biotech) secondary antibodies. Immunoblots were visualized using the Millipore ECL Western Blotting Detection System (Millipore, Billerica, MA, USA). Expression levels were normalized against β-actin (1:5000, Boster Biotech) or Lamin B1 (1:3,000, Cell Signaling Technology).

### **Nissl staining**

Cortical tissue from lesioned areas was fixed in formaldehyde, embedded in paraffin, and cut into 4-µm sections. Slices went through xylene dewaxing and an alcohol gradient rehydration as above and were stained with Nissl solution (Boster Biotech, Wuhan, China) for 5 min. Compared to normal neurons, the cell bodies of injured neurons were shrunken and/or contained vacuoles and the nuclei stained darker. A pathologist who was blinded to the experiments randomly selected five random regions of interest (ROIs) under a high magnification optical microscope (×400; Leica, Wetzlar, Germany) to observe positively stained cells surrounding injured areas. Five random ROIs were selected for quantification, and the mean (%) was used for the statistical analysis.

### **TUNEL staining**

A TUNEL assay was performed using an apoptosis kit according to the manufacturer's instructions (Roche Inc., Indianapolis, IN, USA). Slices were incubated with NeuN (1:500; Abcam) overnight at 4 °C, and after washing in PBS, the samples were incubated with TUNEL reaction mixture for 1 h at 37 °C. TUNEL-positive neurons around the injured area were observed and counted with a microscope at high magnification (×400). Five ROIs were selected for quantification and averaged for statistical analysis.

### **Assessment of neurological injury**

Nerve injury was assessed by modified neurological severity score (mNSS) and Garcia test[22, 42]. The mNSS included motor, sensory, and reflex tests in mice. The neurological injury was recorded when a task was not completed successfully or when the corresponding reflex was lost. The mNSS test was graded on a scale of 0–18, in which a score of 0 indicated normal performance and a total score of 18 points indicated severe neurological deficits, 1–6 indicated mild injury, 7–12 indicated mean-moderate injury,

and 13–18 indicated severe injury. The Garcia test consisted of seven evaluations: spontaneous activity, axial sensation, vibrissae proprioception, and limb symmetry, as well as the ability to perform lateral turning, forelimb outstretching, and climbing. Each test received a score between 0 (worst performance) and 3 (best performance), and a total Garcia score was calculated as the sum of all subtests (maximum = 21 points). The evaluation was performed pre-injury and post-injury (24, 48, and 72 h) by investigators who were blinded to the experiments.

### **Evans blue (EB) extravasation assay**

BBB permeability was investigated by measuring the extravasation of EB. EB (Sigma-Aldrich; 2% in saline; 5 mL/kg) was injected via the common carotid artery 2 h prior to sacrifice 72 h after TBI[15]. Mice were transcardially perfused with ice-cold PBS (pH 7.2–7.4) immediately after sacrifice, followed by 4% paraformaldehyde in PBS. The brains were then removed, dissected, weighed, and homogenized in 600  $\mu$ l 7.5% (w/v) trichloroacetic acid. The samples were then centrifuged. The absorption of the supernatant was measured using a spectrophotometer at a wavelength of 620 nm. The quantity of Evans blue was calculated according to a standard curve and expressed as micrograms of Evans blue/g of brain tissue.

### **Analysis of cerebral edema**

The wet/dry weight method is used to evaluate brain water content, which is a reliable method for brain edema[15]. Briefly, 72 h post-TBI, brains were rapidly removed from the skull, the brain tissue was removed from the injured side with a fixed weight and put in the pre-weighed aluminum foil, and samples were then placed in an oven for 72 h at 90 °C and reweighed for dry weight content. Brain water content was calculated according to the following formula: brain water content (%) = (total wet weight of brain - dry weight of brain)/total wet weight of brain  $\times$  100%.

### **Laser speckle contrast imaging (LSCI)**

Cortical blood flow was monitored using the laser speckle technique as described previously[43]. The laser speckle imaging system (Wuhan SIM Opto-technology Co., Wuhan, China) consisted of a continuous wavelength ( $\lambda$  = 785 nm) laser source, an Olympus ZS61 microscope, a charge-coupled-device camera, and a computer. The selection of the ROIs in the LSCI was performed by tools provided by the software, and the values obtained were the average blood-flow values in the region. Before making the model, the regional CBF was recorded as baseline. LSCI was used to observe the relative blood flow values in the capillary areas surrounding the impinging lesion in mice before and after craniotomy, and post-injury (5 min, 24 h, 72 h). Before inducing the model, the regional CBF was recorded as the baseline.

### **Statistical analysis**

All statistical analyses were performed using SPSS 23.0 statistical software (SPSS Inc., Chicago, IL, USA). The results are expressed as mean  $\pm$  standard deviation. The comparison between two groups was performed using an independent samples t-test, while the statistical difference between each group was

evaluated by one-way analysis of variance (ANOVA) with Bonferroni correction for *post hoc* multiple comparisons. Differences with  $p < 0.05$  were considered statistically significant.

## Results

### **Trauma induces microglial activation and promotes neuroinflammation and oxidative stress.**

Microglia are a major source of inflammatory factors in the brain, and decades of studies have confirmed that microglia are the key driver of the inflammatory response in CNS diseases[6]. At 72 h after TBI, immunohistochemistry showed that the microglial marker Iba-1 increased significantly, suggesting that trauma induced microglial activation and proliferation (Fig. 1a). The expression levels of inflammatory factors (TNF- $\alpha$ , IL-1 $\beta$ , IL-6, IFN- $\gamma$ ) were measured after TBI using ELISA kits, and results showed that the TBI group had significantly higher expression levels of inflammatory factors compared to the control group (Fig. 1b). In addition, we found that the concentrations of ROS and RNS were also significantly increased after TBI (Fig. 1c). These results suggested that microglia were activated after TBI, accompanied by inflammation and oxidative stress.

Neuroinflammation and oxidative damage secondary to TBI are positively correlated with TNF- $\alpha$ [26]. Here, we evaluated the changes of the downstream NF- $\kappa$ B/iNOS pathway by immunohistochemistry. As expected, compared with the control group, TBI up-regulated the expression of NF- $\kappa$ B p65 and iNOS, suggesting that there was NF- $\kappa$ B/iNOS axis activation. ADAM17, also known as TNF- $\alpha$  converting enzyme, is the trigger of TNF- $\alpha$  pro-inflammatory activity[28]. Our results showed that the expression of ADAM17 around the injury areas in the TBI group was also increased (Fig. 1d–g). These results further suggested that TNF- $\alpha$  and its signaling pathway may be closely related to the secondary injury following TBI.

### **Activated microglia release TNF- $\alpha$ and induce the activation of the NF- $\kappa$ B/iNOS signaling axis.**

From the above experimental findings, we found that TNF- $\alpha$ /NF- $\kappa$ B/iNOS axis activation may play an important role in the secondary injury of TBI. However, it is unclear whether this axis is associated with activated microglia, so we further explored the relationship between them in microglia (BV2 cells) cultured *in vitro*. After 24 h of LPS stimulation, immunofluorescence staining showed a significant rise in TNF- $\alpha$  expression levels in BV2 cells (Fig. 2a). Meanwhile, the ELISA results showed that the concentration of TNF- $\alpha$  in the supernatant of the culture medium also increased (Fig. 2b). Subsequently, we determined the degree of activation of the NF- $\kappa$ B/iNOS axis in activated BV2 cells. Western blot analyses revealed that LPS stimulation resulted in phosphorylation of NF- $\kappa$ B p65 and increased the expression of NF- $\kappa$ B p65 and iNOS (Fig. 2c). These results suggested that microglia activated the NF- $\kappa$ B/iNOS pathway by generating TNF- $\alpha$  after LPS stimulation.

### **Blocking TNF- $\alpha$ can play a neuroprotective role in the acute phase of TBI.**

TNF- $\alpha$  is a multifunctional proinflammatory cytokine, and blocking TNF- $\alpha$  is neuroprotective after TBI[27]. Our results suggested that this protective effect may be associated with the inhibition of the TNF- $\alpha$ /NF- $\kappa$ B/iNOS axis. Therefore, we tested our hypothesis by inhibiting TNF- $\alpha$  using IFX. IFX, an anti-TNF- $\alpha$  agent, is a monoclonal antibody that binds to TNF- $\alpha$ [26]. Compared with the TBI group, the expression of TNF- $\alpha$  in microglia was significantly inhibited by IFX (Fig. 3a). Meanwhile, immunofluorescence staining and western blot analysis showed that IFX treatment could inhibit the phosphorylation and nuclear translocation of p65, and reduce the expression of iNOS (Fig. 3b–e), and this result further confirmed the association between TNF- $\alpha$  and the downstream NF- $\kappa$ B/iNOS pathway. Moreover, the ELISA results indicated that the concentrations of inflammatory factors (TNF- $\alpha$ , IL-1 $\beta$ , IL-6, and IFN- $\gamma$ ) and free radicals (ROS, RNS) in the TBI+IFX group were significantly decreased compared to the TBI group at 72 h after TBI (Fig. 3f, g). Excess NO produced by iNOS can quickly react with superoxide anions to form another powerful free radical, peroxynitrite[37, 44, 45]. Here, we determined the expression of 3-NT to laterally reflect peroxynitrite levels[45]. Western blot analysis showed that the expression of 3-NT was significantly increased after TBI, suggesting that the nitric oxide-mediated tyrosine nitrosylation of protein tyrosine residues mediated by peroxynitrite increased, and IFX treatment could down-regulate its expression (Fig. 3e).

Then, we used Nissl staining to assess the damage in neurons. At 72 h after injury, the percentage of injured cells in the TBI group was significantly higher than that in the control group (Fig. 4a). TUNEL staining was used to evaluate the apoptosis of neurons. The results demonstrated that TUNEL-positive neurons were increased in the TBI group compared to the control group (Fig. 4b). Western blot analyses further revealed that TBI resulted in the upregulation of apoptotic factors (cleaved caspase3, Bax) in the cortex 72 h after TBI, whereas the anti-apoptotic factor, Bcl-2, was decreased (Fig. 4c). However, these phenomena were reversed to a certain extent by IFX, indicating that inhibition of TNF- $\alpha$  was beneficial for improving neuronal injury and apoptosis (Fig. 4a–c). We used mNSS and the Garcia test to assess neurological function in all groups. The degree of neurological deficit in the TBI group was the highest 24 h after injury and gradually recovered with time. At 72 h after injury, the neurological function in the TBI+IFX group was significantly improved when compared with the TBI group (Fig. 4d). These results supported our hypothesis that blocking TNF- $\alpha$  after TBI could play a neuroprotective role in the acute phase of injury by reducing neuroinflammation and oxidative stress, and this protective effect was associated with the inhibition of the NF- $\kappa$ B/iNOS pathway.

### **Neuroinflammation and oxidative stress secondary to TBI induce pericyte degeneration.**

We aimed to understand the effect of TBI on pericytes by detecting the changes in pericyte markers. Immunofluorescence imaging analysis of the pericyte marker  $\alpha$ -SMA showed that  $\alpha$ -SMA and endothelial cells (CD31) were co-located in cerebral capillaries, as shown in the sections from injured and uninjured mouse cerebral cortices. At the same time, the expression of  $\alpha$ -SMA in the TBI group decreased significantly compared with the control group. Interestingly, the level of  $\alpha$ -SMA in the TBI+IFX group was significantly higher than that in the TBI group (Fig. 5a). Then, we analyzed the expression of  $\alpha$ -SMA and the other pericyte markers PDGFR- $\beta$  and NG2 in the lysates from mouse cerebral cortices using western blot analysis. The data showed that the expression of PDGFR- $\beta$ ,  $\alpha$ -SMA, and NG2 in the TBI+IFX group

was significantly increased compared with that in the TBI group, although it was still lower than that in the control group (Fig. 5b). Our results suggested that pericyte degeneration after TBI was associated with inflammation and oxidative stress mediated by activation of the TNF- $\alpha$ /NF- $\kappa$ B/iNOS signaling axis.

### **Pericyte degeneration mediates the destruction of the BBB and secondary vasogenic edema.**

Pericytes are necessary for the formation of the BBB and are involved in regulating the function and structural integrity of the BBB, including the formation of TJ proteins[15]. We investigated our hypothesis that pericyte degeneration after TBI would impair the expression or formation of TJ proteins. Using triple immunostaining, we analyzed the expression of TJ proteins (occludin and ZO-1) in brain tissue slices and assessed their co-localization with endothelial cells (CD31). Our results confirmed the expression of occludin and ZO-1 were significantly decreased after TBI, and IFX reduced the decrease in proteins caused by trauma (Fig. 6a). Subsequently, we analyzed the expression of TJ proteins including occludin, claudin-5, and ZO-1 by western blot analysis. Similar to the results of the immunofluorescence staining, occludin, claudin-5, and ZO-1 expression levels were increased in the TBI+IFX group compared to the TBI group (Fig. 6b). Next, we further investigated the effect of the reduction in TJ proteins on BBB permeability by measuring the exudation of EB. The results showed that compared with the control group, the exudation of EB significantly increased in the brain tissues at 72 h after injury in the TBI group, but decreased in the TBI+IFX group (Fig. 6c).

After TBI, BBB disruption leads to increased cerebrovascular leakage, resulting in vasogenic edema. AQP4, as the most important water channel protein in the mammalian brain, is closely related to the occurrence of vasogenic brain edema[40]. The results of the western blot analysis showed that AQP4 expression was enhanced after TBI, which was inhibited by IFX (Fig. 6b). In order to further verify the consequences of BBB destruction and high AQP4 expression, we analyzed the water content of damaged brain tissue for 72 h to assess brain edema and compared this with the control group. The results showed that brain water content in the TBI+IFX group was reduced compared with that in the TBI group (Fig. 6d).

### **Pericyte degeneration mediates limited perfusion into the cerebral microcirculation.**

Recent studies suggest that microvessels covered by pericytes play a key role in local cerebral blood flow regulation[14, 46]. LSCI was used to monitor the changes in microcirculation blood flow in mice at different time points. We found that craniotomy caused minor damage to the cortical vessels, which slightly reduced the blood flow of the local microcirculation. In the TBI group, the general cerebral blood flow decreased significantly after impact, especially in the microcirculation around the injury areas. With the extension of time, the microcirculation around the injury areas gradually recovered in each group. In the TBI+IFX group, the microcirculation blood flow around the lesioned areas was improved at 72 h compared with that in the TBI group, which was close to the preinjury level. However, the blood flow values at other time points were not significantly different from those in the TBI group (Fig. 7a–c). This phenomenon is consistent with the determination of cGMP in the affected side of the brain, which is an

important mediator of NO-mediated vasodilation[34, 47]. The cGMP levels in the TBI+IFX group were increased at 72 h compared to the TBI group but remained lower than the control group (Fig. 7d).

## Discussion

The NVU is the minimum unit necessary to maintain the proper function of CNS[10]. Cerebral microcirculation disturbance mediated by pericytes is an important factor of secondary brain injury after TBI, which is closely related to pathological processes such as neuroinflammation and oxidative stress[1, 48]. Using the mouse CCI model, this study proved the importance of neuroinflammation and oxidative stress in the secondary injury following TBI. Inhibition of the inflammatory factor TNF- $\alpha$  can improve the prognosis of TBI. Meanwhile, we explored the effects of neuroinflammation and oxidative stress on pericyte-mediated microcirculation by assessing the TNF- $\alpha$ /NF- $\kappa$ B/iNOS pathway. We clarified that the TNF- $\alpha$ /NF- $\kappa$ B/iNOS signaling axis in microglia affects the cerebral microcirculation by regulating pericyte function and then plays a vital role in the pathological process after TBI.

Pericytes are vascular mural cells in the NVU that play a vital role in the regulation of the microcirculation[13,14,46]. Recent studies in adult and aging brains demonstrated that pericytes are required for BBB integrity, capillary perfusion, and CBF[15]. To investigate the effects of TBI on pericytes, we used a combination of pericyte markers including  $\alpha$ -SMA, PDGFR- $\beta$ , and NG2 to visualize pericyte changes. At 72 h after TBI, the expression levels of  $\alpha$ -SMA, PDGFR- $\beta$ , and NG2 in the injured brain tissue were significantly decreased compared with those in the control group, suggesting the degeneration and loss of pericytes after TBI. It was also accompanied by disruption of TJ proteins (occludin, ZO-1, claudin5), which suggested damage to the BBB. Loss of brain pericyte-endothelium integrity has been shown to increase transendothelial fluid flow and paracellular transport as a result of reduced TJ protein expression, both causing BBB disruption[15]. Further studies showed that the leakage of EB in brain tissue increased in the TBI group, accompanied by the increase of AQP4 expression and brain water content. These results confirmed the damage of the BBB. In order to evaluate the changes of pericyte-mediated microcirculation blood flow after TBI, we used LSCI to monitor cerebral cortex blood perfusion in mice. The results showed that the perfusion of the microcirculation around the injury areas was significantly inhibited after trauma, and gradually recovered with time.

The TNF- $\alpha$ /NF- $\kappa$ B signaling pathway is the most important pathway in the inflammatory response[49]. NF- $\kappa$ B is associated with the expression of numerous cytokines and is involved in the regulation of the inflammatory response, oxidative stress, apoptosis, and other pathological processes[50, 51]. The NF- $\kappa$ B family consists of five structurally related subunits including P50, p52, p65, RelB, and c-Rel. LPS can stimulate c-Rel activation, enhance the binding of c-Rel to the NF- $\kappa$ B site in the iNOS promoter and thus induce iNOS expression[35, 36]. Previous studies have suggested that the activation of the TNF- $\alpha$ /NF- $\kappa$ B/iNOS axis is related to the inflammatory response and oxidative stress[45, 52]. Our findings suggested that inflammation-associated microglia were activated following trauma, accompanied by increased NF- $\kappa$ B phosphorylation and nuclear translocation, and upregulate iNOS expression. Further experiments *in*

*vitro* also confirmed the relationship between the activation of the TNF- $\alpha$ /NF- $\kappa$ B/iNOS axis and inflammation in BV2 cells. These results are consistent with those of a previous study[53].

To verify the pathological mechanisms of TNF- $\alpha$  after TBI, we utilized IFX to antagonize TNF- $\alpha$ . IFX is a monoclonal antibody that binds to TNF- $\alpha$ , and its protective effects including anti-inflammation, anti-oxidative stress, and anti-apoptosis are thought to attenuate the injury caused by hypoxia, ischemia, edema, and vascular changes in the acute phase of TBI[26]. We found that IFX treatment inhibited the expression of TNF- $\alpha$  in microglia and downregulated NF- $\kappa$ B/iNOS pathway activity. At the same time, the expression levels of inflammatory cytokines, free radicals, and 3-NT decreased in the brain, and neuronal injury and apoptosis were reduced, as well as neurological deficits. These results further indicated the critical role of TNF- $\alpha$  in the secondary injury following TBI, which was associated with the activation of the NF- $\kappa$ B/iNOS axis.

A previous report has shown that NF- $\kappa$ B/iNOS pathway activation was involved in mediating pericyte apoptosis[54]. In our study, we found that inhibition of the TNF- $\alpha$ /NF- $\kappa$ B/iNOS axis by IFX could significantly ameliorate pericyte and TJ protein loss, thus contributing to the preservation of the integrity of BBB structure and function. We also measured the content of cGMP in brain tissue at 72 h postinjury, which is a mediator of NO-mediated vasodilation[34, 47]. cGMP-related signaling is one of the pivotal mechanisms by which pericytes regulate blood flow[55, 56]. Through IFX treatment, we found that microcirculatory blood flow was improved to some extent at 72 h after TBI, and cGMP levels were also increased accordingly. What is interesting is that our experimental results are contrary to Lesley's conclusion. Lesley's study based on iNOS knockout mice claims that iNOS plays a positive role in the recovery of CBF after TBI[57]. We speculate that the contradictory conclusions may be related to different means of blood flow measurement, while iNOS knockout may carry other unanticipated effects. Because NO has a complex role, both neuroprotective and neurotoxic, an appropriate concentration of NO can be of benefit in maintaining blood perfusion.

Nevertheless, this study had limitations. First, we explored the impact on pericytes after activation of the TNF- $\alpha$ /NF- $\kappa$ B/iNOS axis in microglia in the context of the NVU, but we ignored the effect of other NVU components. In addition, it remains unclear by which pathway the TNF- $\alpha$ /NF- $\kappa$ B/iNOS axis damaged pericytes, and whether pericytes underwent some specific phenotypic transformation in this process. Therefore, future research should deeply explore the specific mechanisms underlying the activation of the TNF- $\alpha$ /NF- $\kappa$ B/iNOS axis and mediation of pericyte degeneration, as well as the role of other components of the NVU. These questions may be answered using TNF- $\alpha$  or iNOS knockout mice as well as in further *in vitro* experiments.

## Conclusions

In summary, our study demonstrated that pericyte degeneration after TBI mediated microcirculatory disturbance, which was associated with neuroinflammation and oxidative stress mediated by activation of the TNF- $\alpha$ /NF- $\kappa$ B/iNOS signaling axis in microglia. The inhibition of TNF- $\alpha$  affected the activity of this

signaling axis, thus reducing neuroinflammation and oxidative damage, ultimately protecting cerebral microcirculatory perfusion and BBB integrity and promoting neurological functional repair. Our study proposed a possible mechanism of pericyte-mediated microcirculation dysfunction after TBI, which provided rationale for targeting pericyte as a new therapeutic target.

## Abbreviations

NVU: neurovascular unit; TBI: Traumatic brain injury; TNF- $\alpha$ : Tumor necrosis factor  $\alpha$ ; NF- $\kappa$ B: nuclear factor- $\kappa$ B; CCI: controlled cortical impact; iNOS: inducible nitric oxide synthase; IFX: infliximab; LSCI: Laser speckle contrast imaging; ADAM17: a disintegrin and metalloproteinase 17; LPS: Lipopolysaccharide; CNS: central nervous system; BBB: blood brain barrier; CBF: cerebral blood flow; ROS: reactive oxygen species; RNS: reactive nitrogen species; Iba: ionized calcium-binding adapter molecule; TUNEL: Terminal deoxynucleotidyl transferase dUTP nick-end labeling;  $\alpha$ -SMA:  $\alpha$ -smooth muscle actin; DAPI: 4',6-diamidino-2-phenylindole; IL: Interleukin; IFN: Interferon; cGMP: cyclic guanosine monophosphate; 3-NT: 3-Nitrotyrosine; PDGFR: platelet derived growth factor receptor; NG: neuron-glia; AQP: aquaporin; ELISA: Enzyme-linked immunosorbent assay; mNSS: Modified neurological severity scores; EB: evans blue; ROIs: regions of interest; PBS: phosphate buffered saline; BSA: bovine serum albumin; RIPA: radioimmunoprecipitation assay; ANOVA: one-way analysis of variance.

## Declarations

### Acknowledgments

Sincere appreciation is also given to the teachers and our colleagues from the 900th Hospital, who participated in this study with great cooperation.

### Authors' contributions

Z. and C.W; conception and design, writing of the manuscript. L.L., S.M., H.L and X.H.; supported several experiments, acquisition of data, analysis and interpretation of data. X.C. and S.W.; technical support, obtaining offunding, conception and design, revision of the manuscript. All authors read and approved the final manuscript.

### Funding

This work was supported by the funds from the Fujian Province Scientific Foundation (No. 2019J01168) from Dr. Xiangrong Chen and the Innovation Joint Fund Project of Fujian Province, China (No. 2019Y9045) from Dr. Shousen Wang.

### Availability of data and materials

The datasets analyzed during the current study are available from the corresponding author on reasonable request.

## Ethics approval and consent to participate

The experimental protocols in the present study including all the surgical procedures and animal usages conformed to the guidelines for the care and use of laboratory animals by the National Institutes of Health (NIH) and were approved by the 900th Hospital Ethics Committee (Fuzhou, China).

## Consent for publication

Consent for publication is not applicable for this manuscript.

## Competing interests

The authors declare that they have no competing interests.

## Author details

<sup>a</sup>Department of Neurosurgery, Fuzong Clinical Medical college, Fujian Medical University, Fuzhou 350025, Fujian Province, China. <sup>b</sup>Department of Neurosurgery, the First Affiliated Hospital of Wannan Medical College, Wuhu 241000, Anhui Province, China. <sup>c</sup>Department of Neurosurgery, 900th Hospital, Fuzhou 350025, Fujian Province, China. <sup>d</sup> Department of Neurosurgery, the Second Affiliated Hospital, Fujian Medical University, Quanzhou 362000, Fujian Province, China.

## References

1. Abdul-Muneer PM, Chandra N, Haorah J. Interactions of oxidative stress and neurovascular inflammation in the pathogenesis of traumatic brain injury. *Mol Neurobiol.* 2015;51:966-79.
2. von Leden RE, Yauger YJ, Khayrullina G, Byrnes KR. Central nervous system injury and nicotinamide adenine dinucleotide phosphate oxidase: oxidative stress and therapeutic targets. *J Neurotrauma.* 2017;34:755-64.
3. Ladak AA, Enam SA, Ibrahim MT. A review of the molecular mechanisms of traumatic brain injury. *World Neurosurg.* 2019;131:126-32.
4. Logsdon AF, Lucke-Wold BP, Turner RC, Huber JD, Rosen CL, Simpkins JW. Role of microvascular disruption in brain damage from traumatic brain injury. *Compr Physiol.* 2015;5:1147-60.
5. Zhou Y, Chen Q, Wang Y, Wu H, Xu W, Pan Y, et al. Persistent neurovascular unit dysfunction: pathophysiological substrate and trigger for late-onset neurodegeneration after traumatic brain injury. *Front Neurosci.* 2020;14:581.
6. Liu LR, Liu JC, Bao JS, Bai QQ, Wang GQ. Interaction of microglia and astrocytes in the neurovascular unit. *Front Immunol.* 2020;11:1024.
7. Mäe M, Armulik A, Betsholtz C. Getting to know the cell-cellular interactions and signaling at the neurovascular unit. *Curr Pharm Des.* 2011;17(26):2750-4.

8. Lok J, Wang XS, Xing CH, Maki TK, Wu LM, Guo SZ, et al. Targeting the neurovascular unit in brain trauma. *CNS Neurosci Ther.* 2015;21:304-8.
9. Perez EJ, Tapanes SA, Loris ZB, Balu DT, Sick TJ, Coyle JT, et al. Enhanced astrocytic d-serine underlies synaptic damage after traumatic brain injury. *J Clin Invest.* 2017;127:3114-25.
10. Sweeney MD, Ayyadurai S, Zlokovic BV. Pericytes of the neurovascular unit: key functions and signaling pathways. *Nat Neurosci.* 2016;26;19(6):771-83.
11. Cho H, Seo JH, Wong KH, Terasaki Y, Park J, Bong K, Arai K, Lo EH, Irimia D. Three-dimensional blood-Brain barrier model for in vitro studies of neurovascular pathology. *Sci Rep.* 2015;5:15222.
12. Sandsmark DK, Bashir A, Wellington CL, Diaz-Arrastia R. Cerebral microvascular injury: a potentially treatable endophenotype of traumatic brain injury-induced neurodegeneration. *Neuron.* 2019;103:367-79.
13. Attwell D, Mishra A, Hall CN, O'Farrell FM, Farrell FM, Dalkara T. What is a pericyte. *J Cereb Blood Flow Metab.* 2016;36:451-5.
14. Brown LS, Foster CG, Courtney JM, King NE, Howells DW, Sutherland BA. Pericytes and neurovascular function in the healthy and diseased brain. *Front Cell Neurosci.* 2019;13:282.
15. Bhowmick S, D'Mello V, Mello V, Caruso D, Wallerstein A, Abdul-Muneer PM. Impairment of pericyte-endothelium crosstalk leads to blood-brain barrier dysfunction following traumatic brain injury. *Exp Neurol.* 2019;317:260-70.
16. Zehendner CM, Sebastiani A, Hugonnet A, Bischoff F, Luhmann HJ, Thal SC. Traumatic brain injury results in rapid pericyte loss followed by reactive pericytosis in the cerebral cortex. *Sci Rep.* 2015;5:13497.
17. Dore-Duffy P, Wang S, Mehedi A, Katyshev V, Cleary K, Tapper A, et al. Pericyte-mediated vasoconstriction underlies TBI-induced hypoperfusion. *Neurol Res.* 2011;33:176-86.
18. Osipova ED, Semyachkina-Glushkovskaya OV, Morgun AV, Pisareva NV, Malinovskaya NA, Boitsova EB, et al. Gliotransmitters and cytokines in the control of blood-brain barrier permeability. *Rev Neurosci.* 2018;29:567-91.
19. Wu KC, Lee CY, Chou FY, Chern Y, Lin CJ. Deletion of equilibrative nucleoside transporter-2 protects against lipopolysaccharide-induced neuroinflammation and blood-brain barrier dysfunction in mice. *Brain Behav Immun.* 2020;84:59-71.
20. Kumar A, Henry RJ, Stoica BA, Loane DJ, Abulwerdi G, Bhat SA, et al. Neutral sphingomyelinase inhibition alleviates LPS-induced microglia activation and neuroinflammation after experimental traumatic brain injury. *J Pharmacol Exp Ther.* 2019;368:338-52.
21. Wang W, Zinsmaier AK, Firestone E, Lin R, Yatskievych TA, Yang S, et al. Blocking tumor necrosis factor-alpha expression prevents blast-induced excitatory/inhibitory synaptic imbalance and parvalbumin-positive interneuron loss in the hippocampus. *J Neurotrauma.* 2018;35:2306-16.
22. Chen X, Chen C, Fan S, Wu S, Yang F, Fang Z, et al. Omega-3 polyunsaturated fatty acid attenuates the inflammatory response by modulating microglia polarization through SIRT1-mediated

- deacetylation of the HMGB1/NF- $\kappa$ B pathway following experimental traumatic brain injury. *J Neuroinflammation*. 2018;15:116.
23. Thurgur H, Pinteaux E. Microglia in the neurovascular unit: blood-brain barrier-microglia interactions after central nervous system disorders. *Neuroscience*. 2019;1;405:55-67.
  24. Sankar SB, Pybus AF, Liew A, Sanders B, Shah KJ, Wood LB, et al. Low cerebral blood flow is a non-invasive biomarker of neuroinflammation after repetitive mild traumatic brain injury. *Neurobiol Dis*. 2019;124:544-54.
  25. Joost E, Jordão M, Mages B, Prinz M, Bechmann I, Krueger M. Microglia contribute to the glia limitans around arteries, capillaries and veins under physiological conditions, in a model of neuroinflammation and in human brain tissue. *Brain Struct Funct*. 2019;224:1301-14.
  26. Zhou Y, Fan R, Botchway B, Zhang Y, Liu X. Infliximab can improve traumatic brain injury by suppressing the tumor necrosis factor alpha pathway. *Mol Neurobiol*. 2021;58:2803-11.
  27. Pooladanda V, Thatikonda S, Bale S, Pattnaik B, Sigalapalli DK, Bathini NB, et al. Nimbolide protects against endotoxin-induced acute respiratory distress syndrome by inhibiting TNF- $\alpha$  mediated NF- $\kappa$ B and HDAC-3 nuclear translocation. *Cell Death Dis*. 2019;10:81.
  28. Düsterhöft S, Lokau J, Garbers C. The metalloprotease ADAM17 in inflammation and cancer. *Pathol Res Pract*. 2019;215:152410.
  29. Kalliolias GD, Ivashkiv LB. TNF biology, pathogenic mechanisms and emerging therapeutic strategies. *Nat Rev Rheumatol*. 2016 Jan;12(1):49-62.
  30. Muballe KD, Sewani-Rusike CR, Longo-Mbenza B, Iputo J. Predictors of recovery in moderate to severe traumatic brain injury. *J Neurosurg*. 2018:1-10.
  31. Gomez A, Serrano A, Salero E, Tovar A, Amescua G, Galor A, et al. Tumor necrosis factor-alpha and interferon-gamma induce inflammasome-mediated corneal endothelial cell death. *Exp Eye Res*. 2021:108574.
  32. Chen X, Famurewa AC, Tang J, Olatunde OO, Olatunji OJ. Hyperoside attenuates neuroinflammation, cognitive impairment and oxidative stress via suppressing TNF- $\alpha$ /NF- $\kappa$ B/caspase-3 signaling in type 2 diabetes rats. *Nutr Neurosci*. 2021;16:1-11.
  33. Okada T, Teranishi K, Chen Y, Tomori T, Strasser A, Lenz FA, et al. Reversal of postischemic hypoperfusion by tempol: Endothelial signal transduction mechanism. *Neurochem Res*. 2012;37:680-8.
  34. Toda N, Ayajiki K, Okamura T. Cerebral blood flow regulation by nitric oxide: Recent advances. *Pharmacol Rev*. 2009;61:62-97.
  35. Hu YC, Sun Q, Li W, Zhang DD, Ma B, Li S, et al. Biphasic activation of nuclear factor kappa B and expression of p65 and c-Rel after traumatic brain injury in rats. *Inflamm Res*. 2014;63:109-15.
  36. Hwang SY, Hwang JS, Kim SY, Han IO. O-GlcNAcylation and p50/p105 binding of c-Rel are dynamically regulated by LPS and glucosamine in BV2 microglia cells. *Br J Pharmacol*. 2013;169:1551-60.

37. Madan S, Kron B, Jin Z, Al Shamy G, Campeau PM, Sun Q, et al. Arginase overexpression in neurons and its effect on traumatic brain injury. *Mol Genet Metab*. 2018;125:112-7.
38. Yemisci M, Gursoy-Ozdemir Y, Vural A, Can A, Topalkara K, Dalkara T. Pericyte contraction induced by oxidative-nitrative stress impairs capillary reflow despite successful opening of an occluded cerebral artery. *Nat Med*. 2009;15:1031-7.
39. Hall CN, Reynell C, Gesslein B, Hamilton NB, Mishra A, Sutherland BA, O'Farrell FM, Buchan AM, Lauritzen M, Attwell D. Capillary pericytes regulate cerebral blood flow in health and disease. *Nature*. 2014;3;508(7494):55-60.
40. Xiong A, Xiong R, Yu J, Liu Y, Liu K, Jin G, et al. Aquaporin-4 is a potential drug target for traumatic brain injury via aggravating the severity of brain edema. *Burns Trauma*. 2021;9:tkaa050.
41. Nacci C, Leo V, De Benedictis L, Potenza MA, Sgarra L, De Salvia MA, et al. Infliximab therapy restores adiponectin expression in perivascular adipose tissue and improves endothelial nitric oxide-mediated vasodilation in mice with type 1 diabetes. *Vascul Pharmacol*. 2016;87:83-91.
42. Zhang M, Huang LL, Teng CH, Wu FF, Ge LY, Shi YJ, et al. Isoliquiritigenin provides protection and attenuates oxidative stress-induced injuries via the Nrf2-ARE signaling pathway after traumatic brain injury. *Neurochem Res*. 2018;43:2435-45.
43. Wang C, Xian L, Chen X, Li Z, Fang Y, Xu W, et al. Visualization of cortical cerebral blood flow dynamics during craniotomy in acute subdural hematoma using laser speckle imaging in a rat model. *Brain Res*. 2020;1742:146901.
44. Scheschowitsch K, de Moraes JA, Sordi R, Barja-Fidalgo C, Assreuy J. Rapid NOS-1-derived nitric oxide and peroxynitrite formation act as signaling agents for inducible NOS-2 expression in vascular smooth muscle cells. *Pharmacol Res*. 2015;100:73-84.
45. Wang M, Deng J, Lai H, Lai Y, Meng G, Wang Z, et al. Vagus nerve stimulation ameliorates renal ischemia-reperfusion injury through inhibiting NF- $\kappa$ B activation and iNOS protein expression. *Oxid Med Cell Longev*. 2020;2020:7106525.
46. Kisler K, Nelson AR, Rege SV, Ramanathan A, Wang Y, Ahuja A, et al. Pericyte degeneration leads to neurovascular uncoupling and limits oxygen supply to brain. *Nat Neurosci*. 2017;20:406-16.
47. Shvedova M, Litvak MM, Roberts JD Jr, Fukumura D, Suzuki T, Şencan İ, et al. cGMP-dependent protein kinase I in vascular smooth muscle cells improves ischemic stroke outcome in mice. *J Cereb Blood Flow Metab*. 2019;39:2379-91.
48. Wu Y, Wu H, Zeng J, Pluimer B, Dong S, Xie X, et al. Mild traumatic brain injury induces microvascular injury and accelerates Alzheimer-like pathogenesis in mice. *Acta Neuropathol Commun*. 2021;9(1):74.
49. Tuttolomondo A, Pecoraro R, Pinto A. Studies of selective TNF inhibitors in the treatment of brain injury from stroke and trauma: a review of the evidence to date. *Drug Des Devel Ther*. 2014;8:2221-38.
50. Dresselhaus EC, Meffert MK. Cellular specificity of NF- $\kappa$ B function in the nervous system. *Front Immunol*. 2019;10:1043.

51. Shih RH, Wang CY, Yang CM. NF-kappaB signaling pathways in neurological inflammation: a mini review. *Front Mol Neurosci.* 2015;8:77.
52. Matsumoto J, Dohgu S, Takata F, Machida T, Bölükbaşı Hatip FF, Hatip-Al-Khatib I, Yamauchi A, Kataoka Y. TNF- $\alpha$ -sensitive brain pericytes activate microglia by releasing IL-6 through cooperation between I $\kappa$ B-NF $\kappa$ B and JAK-STAT3 pathways. *Brain Res.* 2018;1;1692:34-44.
53. Park T, Chen H, Kevala K, Lee JW, Kim HY. N-Docosahexaenoyl ethanolamine ameliorates LPS-induced neuroinflammation via cAMP/PKA-dependent signaling. *J Neuroinflammation.* 2016;13:284.
54. Kim J, Kim OS, Kim CS, Kim NH, Kim JS. Cytotoxic role of methylglyoxal in rat retinal pericytes: Involvement of a nuclear factor-kappaB and inducible nitric oxide synthase pathway. *Chem Biol Interact.* 2010;188:86-93.
55. Xiao M, Li Q, Feng H, Zhang L, Chen Y. Neural vascular mechanism for the cerebral blood flow autoregulation after hemorrhagic stroke. *Neural Plast.* 2017;2017:5819514.
56. Špiranec K, Chen W, Werner F, Nikolaev VO, Naruke T, Koch F, Werner A, Eder-Negrin P, Diéguez-Hurtado R, Adams RH, et al. Endothelial C-type natriuretic peptide acts on pericytes to regulate microcirculatory flow and blood pressure. *Circulation.* 2018;31;138(5):494-508.
57. Foley LM, Hitchens TK, Melick JA, Bayir H, Ho C, Kochanek PM. Effect of inducible nitric oxide synthase on cerebral blood flow after experimental traumatic brain injury in mice. *J Neurotrauma.* 2008;25:299-310.

## Figures

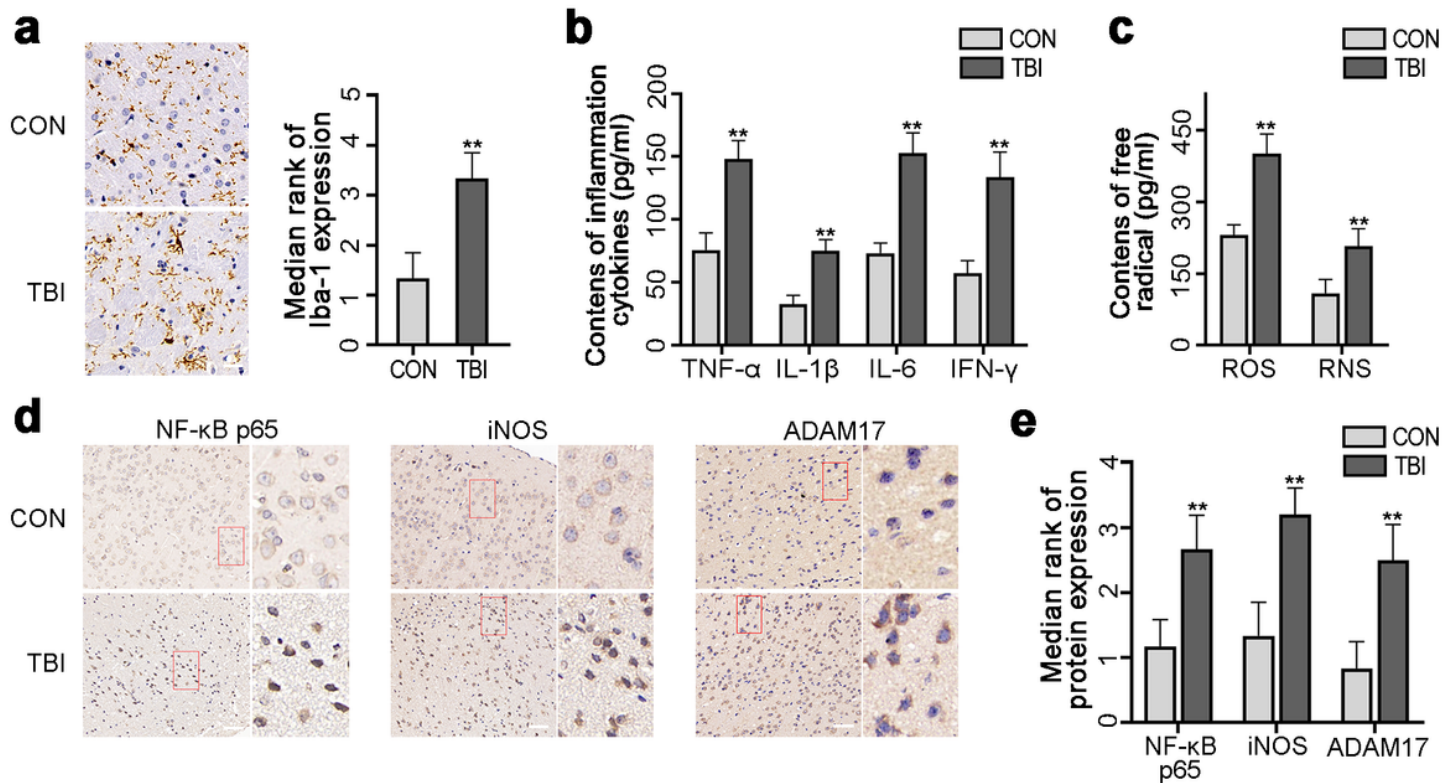


**Figure 1**

TBI induces neuroinflammation and oxidative stress. a The expression of the microglial marker, Iba-1, increased significantly at 72 h after TBI. Scale bars = 20  $\mu$ m. b, c TBI promotes the production of inflammatory factors (TNF- $\alpha$ , IL-1 $\beta$ , IL-6, and IFN- $\gamma$ ) and free radicals (ROS, RNS) around the injury areas. d, e After trauma, the expression of NF- $\kappa$ B p65, iNOS, and ADAM17 increased in the lesioned area. Representative images of immunohistochemical staining of NF- $\kappa$ B p65, iNOS, and ADAM17. Scale bars = 50  $\mu$ m. Values are expressed as the mean  $\pm$  standard deviation (n = 6 per group), \*p < 0.05, \*\*p < 0.01.

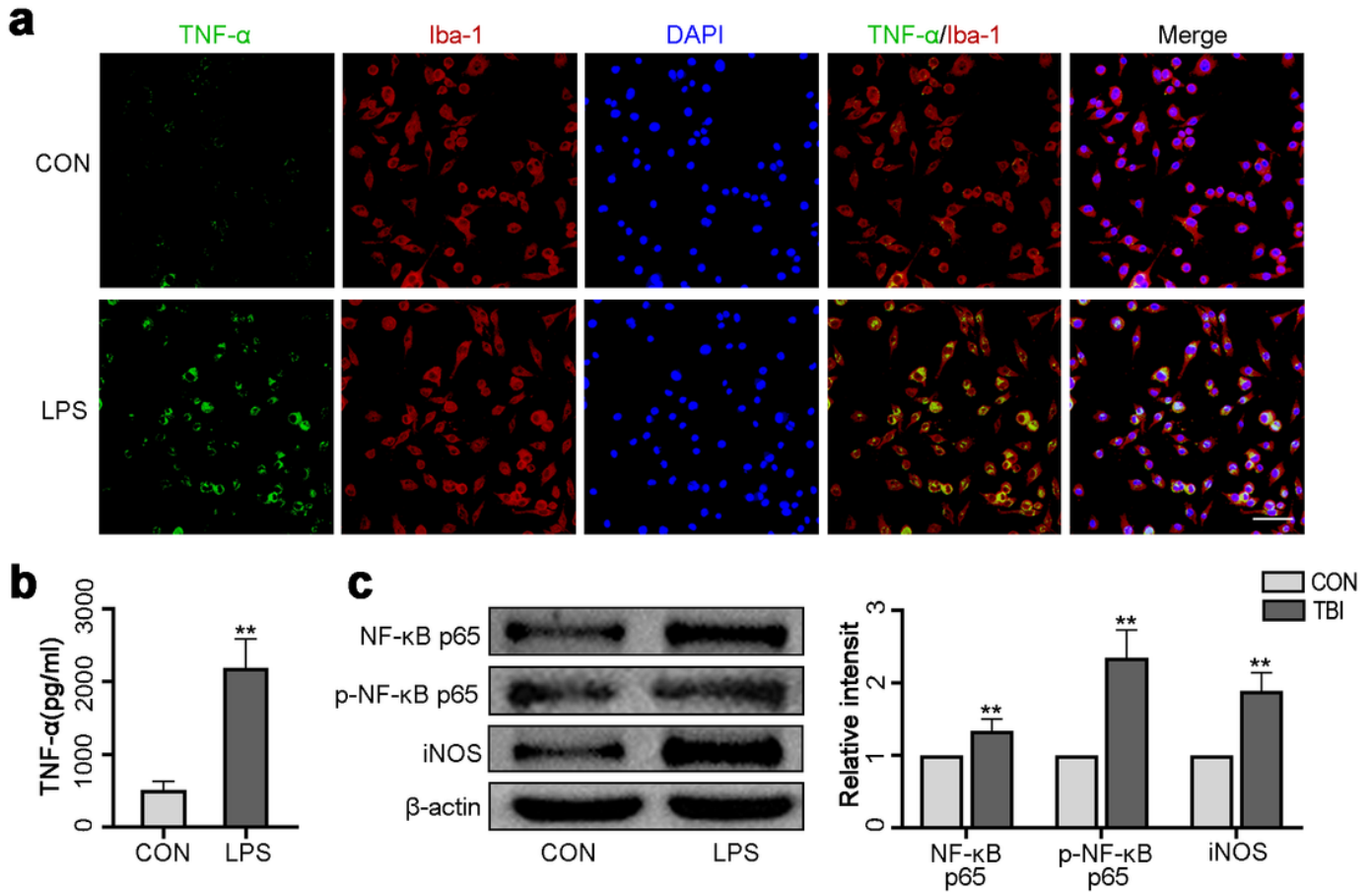


**Figure 2**

Activated microglia upregulate the expression of TNF- $\alpha$ , which promotes NF- $\kappa$ B/iNOS signaling in vitro. a At 24 h after LPS stimulation, BV2 cells (Iba-1+) had increased TNF- $\alpha$  expression. b ELISA showed that the concentration of TNF- $\alpha$  in the culture medium increased significantly after LPS stimulation. c Activation of NF- $\kappa$ B p65 and iNOS in BV2 cells treated with LPS for 24 h. Values are expressed as the mean  $\pm$  standard deviation (n = 6 per group), \*p < 0.05, \*\*p < 0.01. Scale bars = 50  $\mu$ m

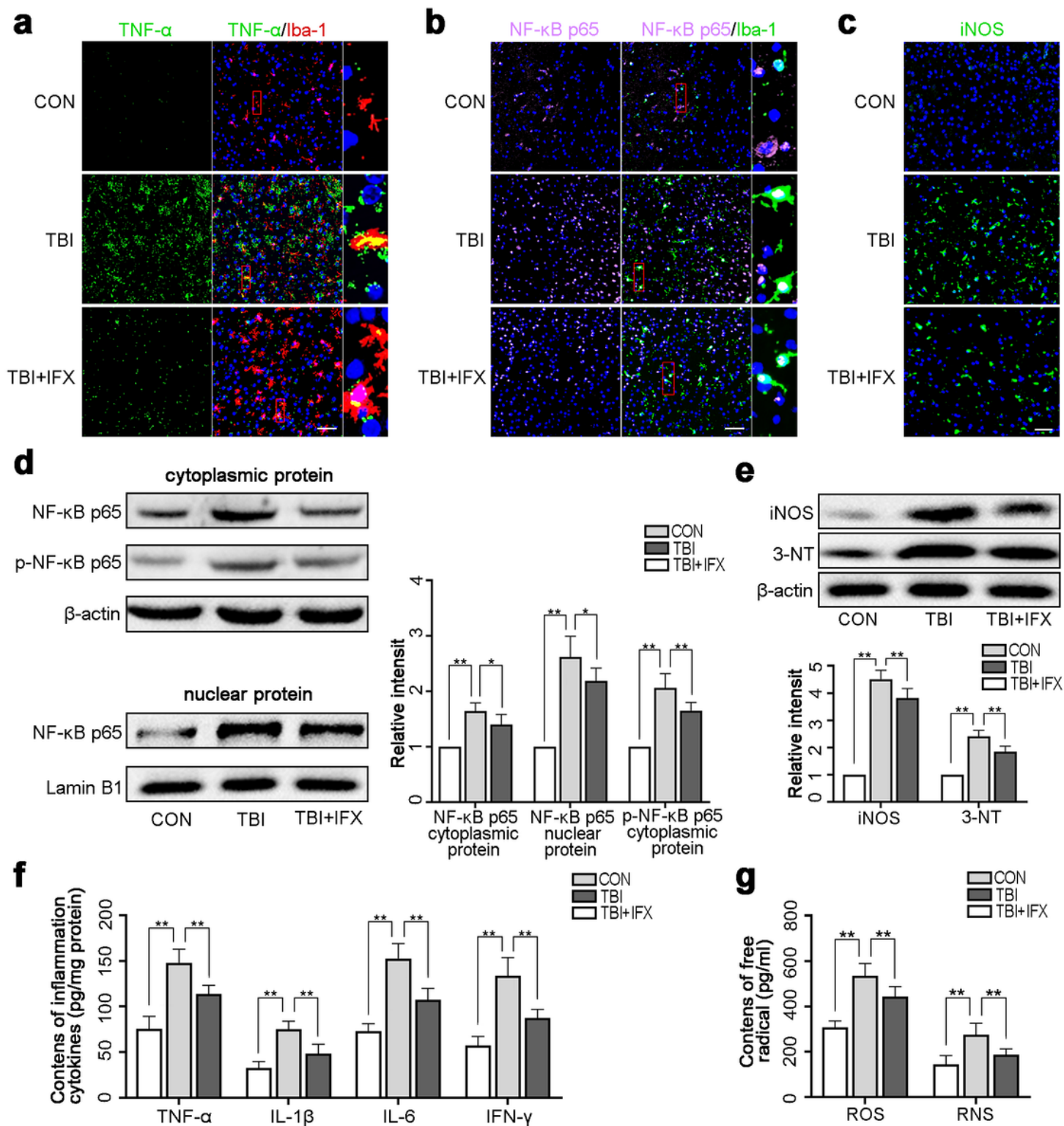


**Figure 3**

IFX reduces neuroinflammation and oxidative damage by inhibiting the activation of the TNF-α/NF-κB/iNOS pathway. a IFX inhibited the expression of TNF-α in microglia (Iba-1+). b Immunofluorescence staining showed that IFX treatment significantly inhibited the nuclear translocation of NF-κB p65 in microglia (Iba-1+). c TBI enhanced the expression of iNOS, which was decreased by IFX supplementation. Representative photomicrographs of iNOS are shown. d IFX supplementation significantly decreased the

expression and phosphorylation of NF- $\kappa$ B p65 and inhibited the translocation of NF- $\kappa$ B p65 from the cytoplasm to the nucleus. e Western blot analyses revealed that TBI resulted in the upregulation of iNOS and 3-NT in the cortex; however, compared with the TBI group, the levels of both were decreased in the TBI+IFX group. f, g ELISA results showed that inhibition of TNF- $\alpha$  could significantly decrease TBI-induced enhancement of inflammatory factors and free radicals. Values are expressed as the mean  $\pm$  standard deviation (n = 6 per group), \*p < 0.05, \*\*p < 0.01. Scale bars = 50  $\mu$ m

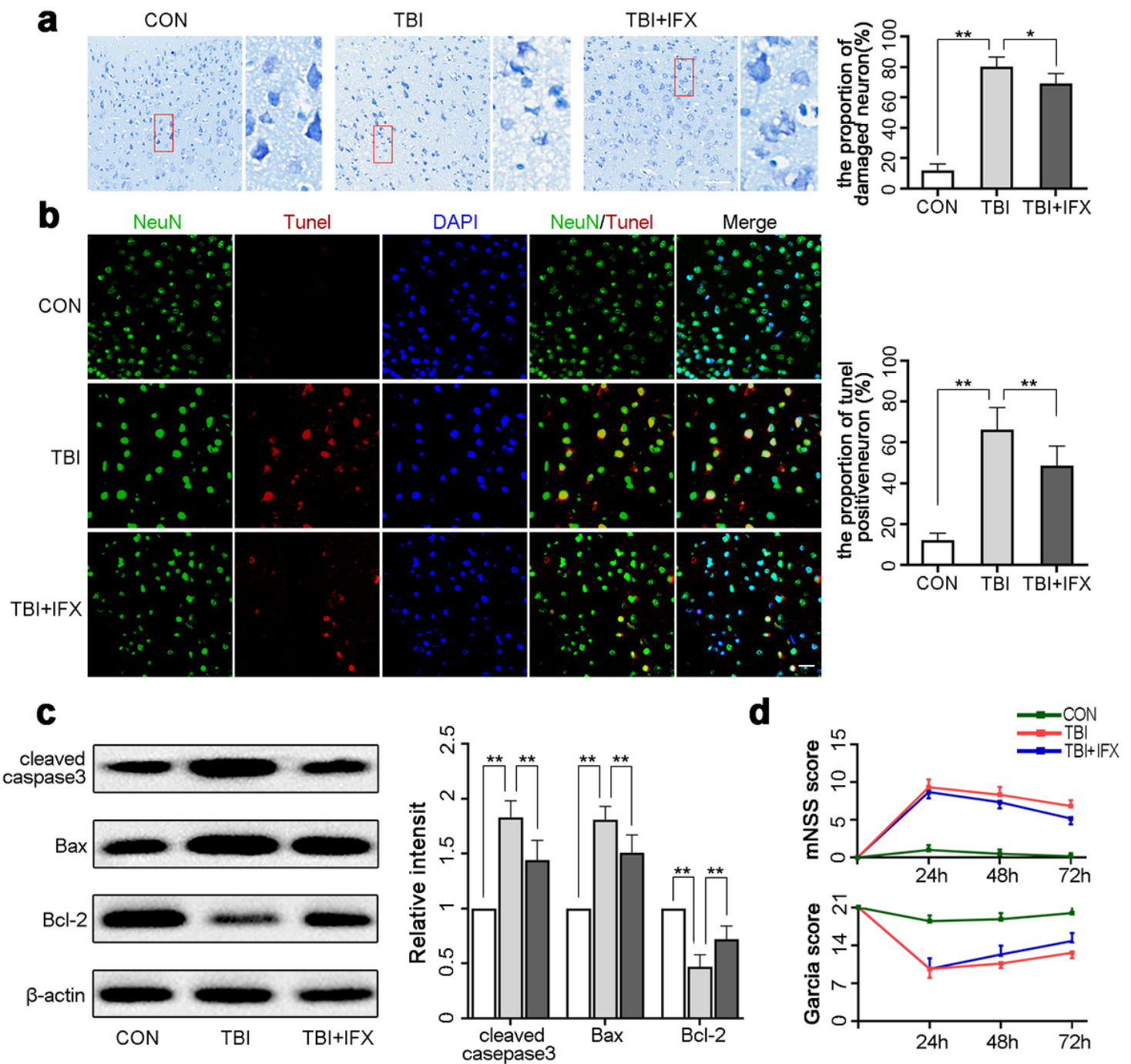


**Figure 4**

Inhibition of TNF- $\alpha$  can play a neuroprotective role after TBI. a The percentage of damaged cells was higher in the TBI group than in the control group; the damaged fraction was significantly lower in the

TBI+IFX group than in the TBI group. Representative photomicrographs of Nissl-stained neurons are shown. Scale bars = 50  $\mu$ m. b IFX supplementation significantly decreased the rate of TUNEL-positive neurons after TBI. Scale bars = 20  $\mu$ m. c Western blot demonstrated that the expression of apoptotic factors (cleaved caspase3 and Bax) was significantly reduced in the TBI+IFX group compared with the TBI group, along with an increase in the anti-apoptotic factor (Bcl-2). d Antagonizing TNF- $\alpha$  ameliorates neurological deficits 72 h after TBI. Values are expressed as the mean  $\pm$  standard deviation (n = 6 per group), \*p < 0.05, \*\*p < 0.01.

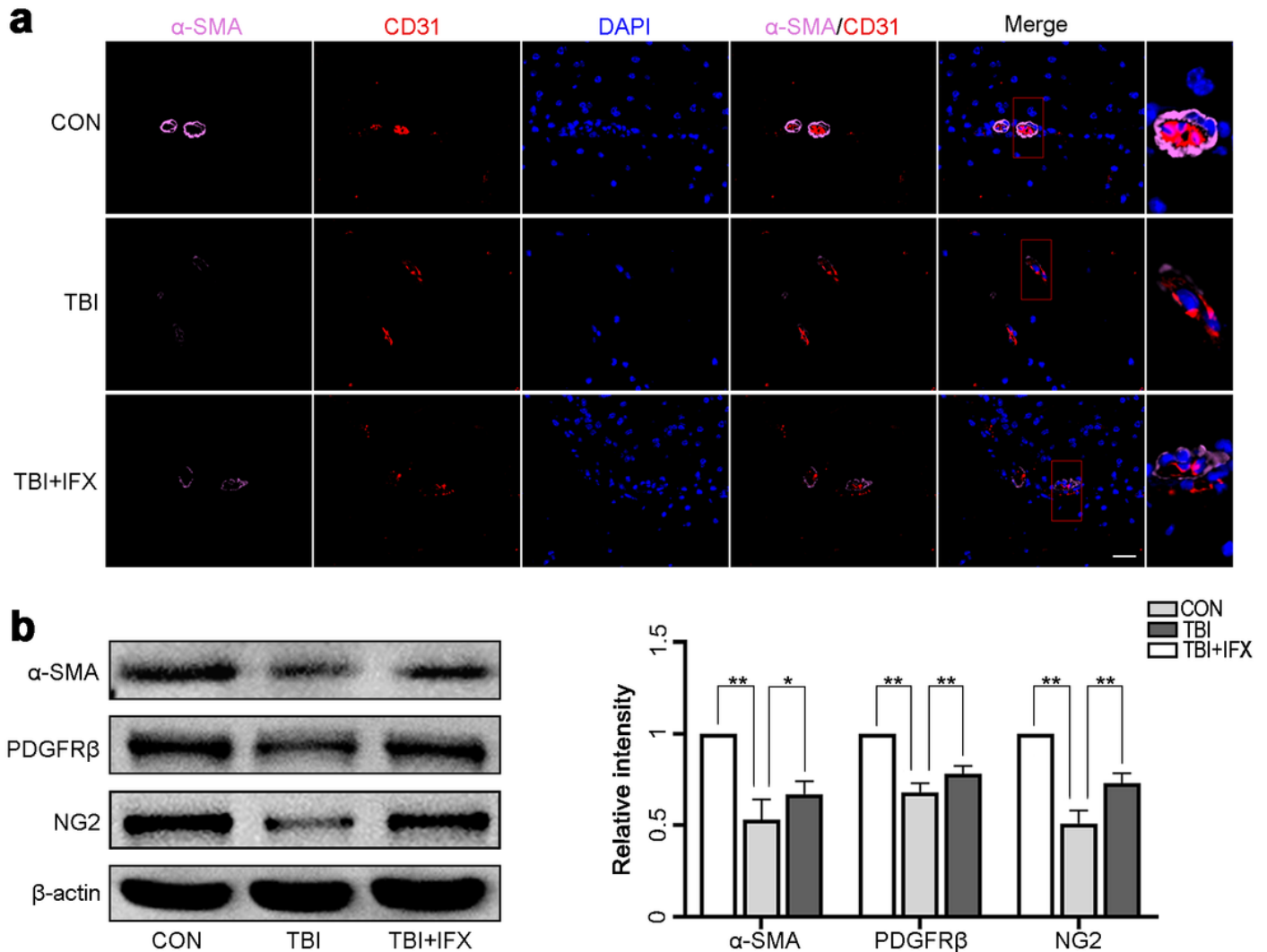


**Figure 5**

TBI results in loss of pericyte coverage. a Immunofluorescent staining of  $\alpha$ -SMA merged with endothelial cells (CD31+) in mouse brain cortex tissue samples of the control, TBI, and TBI+IFX groups at 72 h after injury. b Western blot analysis of  $\alpha$ -SMA, PDGFR- $\beta$ , and NG2 in mouse cortical tissue lysates from the control, TBI, and TBI+IFX injury groups 72 h after TBI. Bar diagram represents the results expressed as a ratio of pericyte markers and  $\beta$ -actin bands. Values are expressed as the mean  $\pm$  standard deviation (n = 6 per group), \*p < 0.05, \*\*p < 0.01. Scale bars = 20  $\mu$ m.

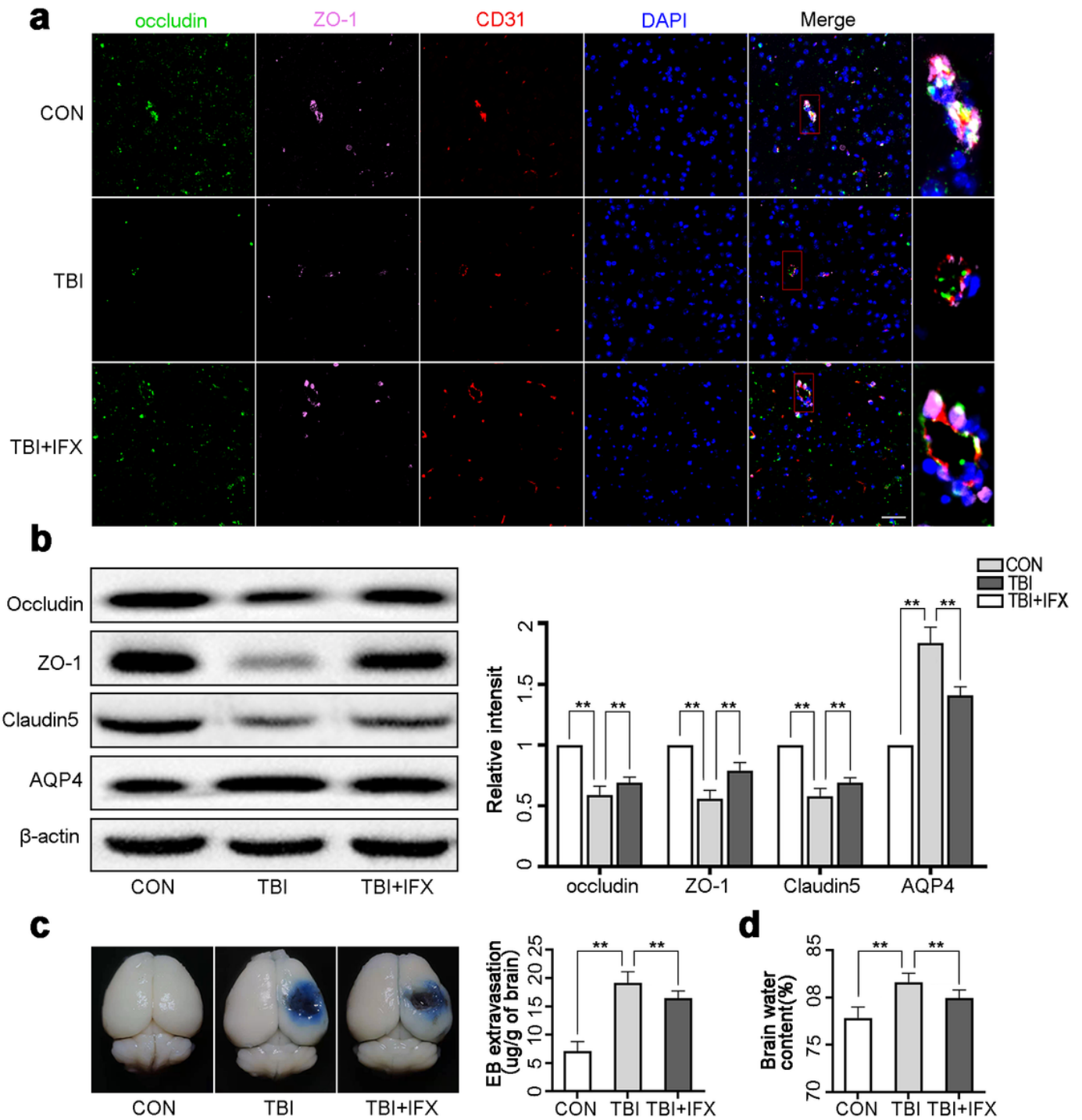


**Figure 6**

TBI destroys the BBB and aggravates brain edema by mediating pericyte degeneration. a Representative images of fluorescent staining of occludin and ZO-1 merged with endothelial cells (CD31+) in mouse brain cortex tissue samples of the control, TBI, and TBI+IFX groups at 72 h after injury. b TJ proteins (occludin, ZO-1, claudin5) and AQP4 in different groups measured by western blot. c The TBI group had more EB extravasation in the brain 72 h after TBI. Compared with the TBI group, the TBI+IFX group had significantly decreased EB extravasation. Representative photos of EB extravasation in the experimental

groups. d Antagonizing TNF- $\alpha$  decreased brain water content 72 h after TBI. Values are expressed as the mean  $\pm$  standard deviation (n = 6 per group), \*p < 0.05, \*\*p < 0.01. Scale bars = 20  $\mu$ m.

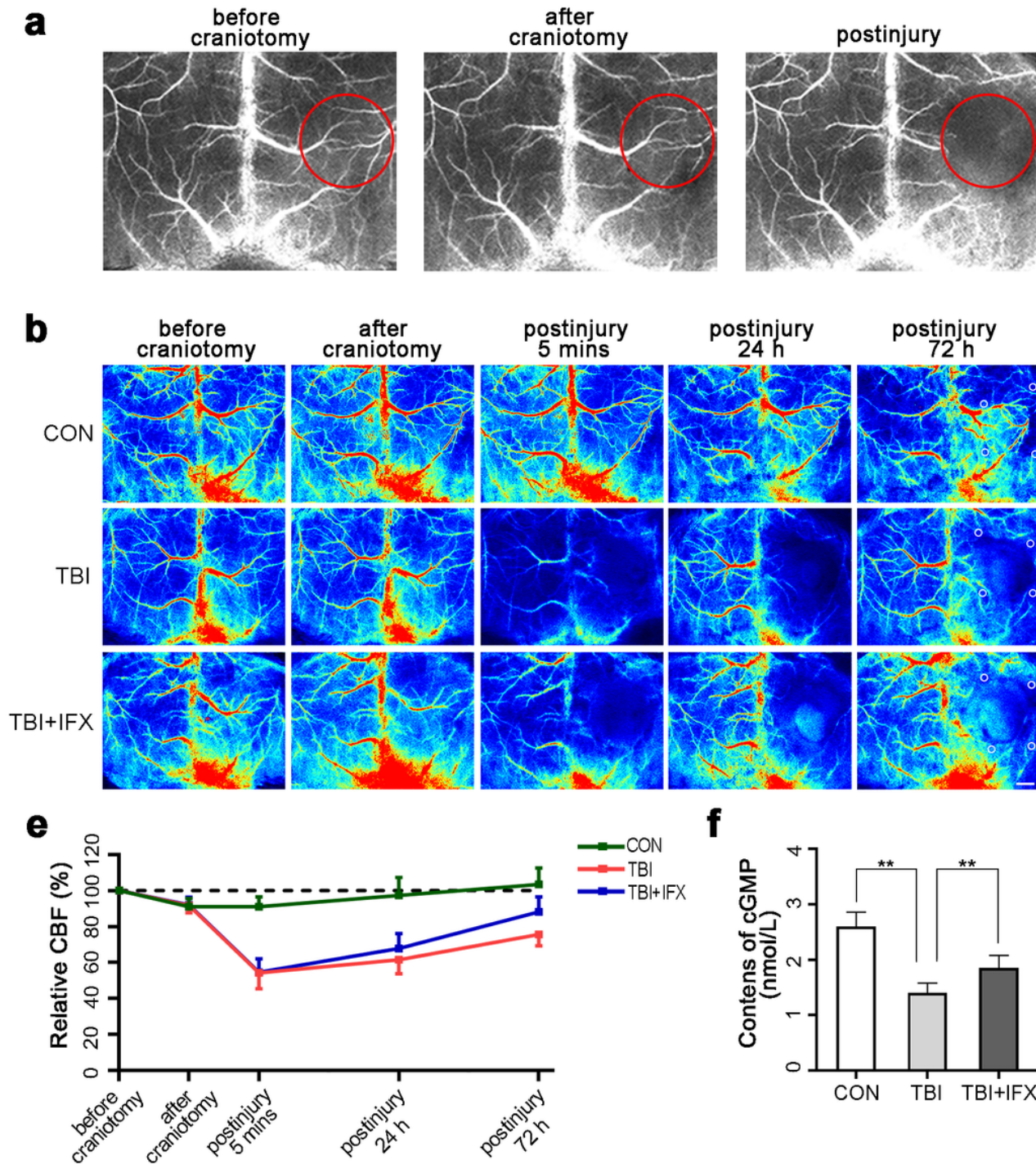


**Figure 7**

Pericyte dysfunction affects microcirculatory blood flow after TBI. a Craniotomy slightly damaged the cortical vessels, while CCI caused severe damage to the vessels in the injured area. The red circle in the figure is the preset strike zone. Scale bars = 0.5 mm. b Representative LSCI blood-flow map at different time points in the control, TBI, and TBI+IFX groups. The white circle marked in the figure is the region of interest (ROI). c After impact, the blood flow in the microcirculation area decreased significantly in the TBI

group, and then gradually recovered. Inhibition of TNF- $\alpha$  could improve local blood flow 72 h after impact, but there was no significant difference at other time points. d The ELISA results showed that the content of cGMP in the TBI+IFX group was significantly higher than that in the TBI group. Values are expressed as the mean  $\pm$  standard deviation (n = 6 per group), \*p < 0.05, \*\*p < 0.01.